ISSN 0554-6397
Originalni znanstveni članak
(*Original scientific paper*)

Vladimir Pelić
E-mail: vpelic@pfri.hr
University of Rijeka, Faculty of Maritime Studies
Studentska ulica 2, 51000 Rijeka, Croatia
Tomislav Mrakovčić
E-mail: tomislav.mrakovcic@riteh.hr
Ozren Bukovac
E-mail: ozren.bukovac@riteh.hr
Marko Valčić
E-mail: marko.valcic@riteh.hr
University of Rijeka, Faculty of Engineering
Vukovarska 58, 51000 Rijeka, Croatia

Development and Validation of 4 Stroke Marine Diesel Engine Numerical Model

Abstract

Increasing demands on energy efficiency and environmental acceptance are being imposed on marine propulsion plants. The fulfilment of the conditions set by the MARPOL Convention, Annex VI, regarding the emissions from exhaust gases of marine diesel engines is of particular interest. This paper presents the development and validation of a zero-dimensional, single-zone diesel engine numerical model. Presented numerical model is based on the law of conservation of energy and mass and solving the resulting differential equations. The single-zone model will serve as the basis for a model where the cylinder space is divided into two or three zones during combustion. In this way, the multi-zone model will allow the modelling of nitrogen oxide emissions with satisfactory accuracy. Validation of the diesel engine model was carried out for the Wärtsilä 12V50DF 11700 kW motor designed to drive a synchronous alternator. Obtained results and deviations of certain parameters in the operation of the engine with respect to the data obtained from the measurements on the test bed, are more than satisfactory regarding complexity of the numerical model. This confirmed the usability of the model for research purposes to optimize the marine diesel engine.

Keywords: diesel engine, numerical modelling, zero-dimensional model

1. Introduction

Transport of goods by waterways is the most efficient and wellknown form of transport concerning energy consumption and total cost per tons of cargo transported. According to UNCTAD data [1] (*United Nations Conference on Trade and Development*) from 2017, there was a global increase in maritime transport of 4.0% and the total quantity of goods transported amounted to 10.7 billion tons. According to UNCTAD forecasts, the total annual growth of maritime transport will continue in the period from 2018 to 2023 with average annual rate of 3.8%.

Regardless of the purpose and size, each ship requires a reliable, economical and environmentally friendly propulsion system. In the merchant fleet, diesel engines are the most frequently used for propulsion. Low-speed diesel engines are heat machines with the highest achieved thermal efficiency, which exceeds 50%. In the medium-speed marine engines, the thermal efficiency is slightly lower and ranges from 45% to 48%. The lower efficiency of 4-stroke diesel engines can be successfully improved by the use of diesel-electric propulsion or by recovering the heat contained in exhaust gases and cooling water. In this context, it is necessary to point out that the exhaust heat exergies of 4-stroke diesel engines are noticeably higher for the higher exhaust gas temperature.

Energy efficiency and environmental acceptability are being placed on the ship's propulsion plants. It is of particular interest to fulfil the conditions set by MARPOL, Annex VI, regarding the emission of harmful substances in the exhaust gases of marine diesel engines.

The research aims to optimise the operation of the diesel engine for the three-phase synchronous generator regarding specific fuel consumption and nitrogen oxide emission. When choosing an engine numerical model, attention was focused on its simplicity, efficiency and satisfactory accuracy of the results obtained in order to quick and easily check the impact of the aforementioned measures on engine performance.

The presented numerical model is based on the law of conservation of energy and mass. The resulting differential equations for main engine components are formed and solved as described in [2] and [3]. The engine numerical model also features additional options such as selecting the integration step, changing the start of the intake valve closure, adjusting the air mass flow through the turbocharger, multiple fuel injection and more.

A computer program is written in C++ programming language. When developing the program, attention is focused towards modularity that makes it easier to check, modify, and upgrade. The final validation of the engine numerical model was carried out using the information provided by the engine manufacturer, data obtained during sea trial, and the test data relating to the Wärtsilä W12V50DF engine with rated power of 11700 kW.

2. Diesel engine numerical model

A single zone zero-dimensional model of four-stroke diesel engine was developed for investigation of the impact of the early intake valve closure (Miller's process), the increase in charging pressure and multiple injections of fuel to specific fuel consumption, pressures and temperatures in the engine cylinder.

Developed model provide analysis of the engine operation in stationary working conditions while engine load is a synchronous three-phase generator.

The four-stroke diesel engine consists of the following main components or control volumes: engine cylinder, intake manifold, exhaust manifold, turbocharger, air cooler, fuel injection subsystems and corresponding crank and valve train mechanisms. The basic diesel engine control volumes covered by the numerical model are shown in Figure 1.

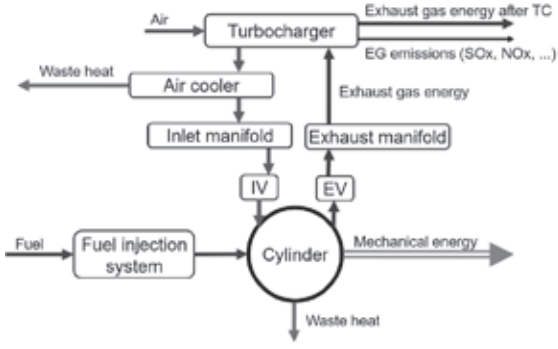

Figure 1: Diesel engine subsystems covered by a numerical model

Engine control volumes are interconnected by connections that enable the exchange of the working media fluid while heat exchange is achieved through their boundaries. The principle of marking engine control volumes and connections between them is shown in Figure 2.

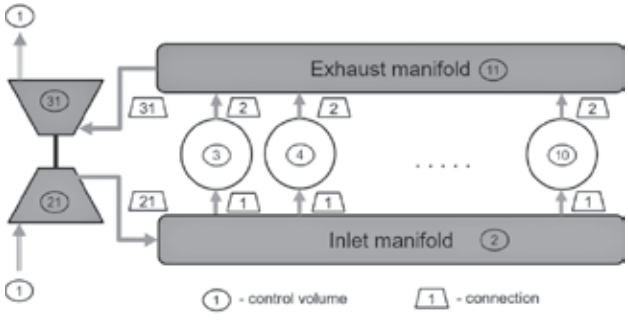

Figure 2: Engine control volumes and connections

The zero-dimensional model presumes a homogeneous mixture of the working fluid with the same temperature and pressure in all parts of the control volume at the observed time or crankshaft position. The current state in control volumes is determined using differential equations derived from the laws of conservation of energy and mass.

2.1. Engine cylinder

During engine operation, chemical energy of the fuel is transformed into thermal energy by fuel combustion in the engine cylinder. It is implied that cylinder walls and piston represent engine cylinder control volume boundaries.

From the law of conservation of mass, change of working fluid mass dm by crankshaft angle dφ follows expression:

$$\frac{\mathrm{d}m_{\mathrm{c}}}{\mathrm{d}\phi} = \frac{\mathrm{d}m_{\mathrm{c,in}}}{\mathrm{d}\phi} + \frac{\mathrm{d}m_{\mathrm{c,out}}}{\mathrm{d}\phi} + \frac{\mathrm{d}m_{\mathrm{c,f}}}{\mathrm{d}\phi} + \frac{\mathrm{d}m_{\mathrm{c,leak}}}{\mathrm{d}\phi} \tag{1}$$

where $m_{\mathrm{c,in}}$ is mass of fluid that enters control volume (engine cylinder), $m_{\mathrm{c,out}}$ is mass of fluid coming out of the control volume, $m_{\mathrm{c,f}}$ is mass of the fuel to be supplied, while $m_{\mathrm{c,leak}}$ is mass of media that exits the control volume due to leakage. In the case of new or regularly maintained engine, a fraction of the mass of media that is lost due to leakage is very small and can be neglected.

The law of conservation of energy in the control volume can be expressed with the following expression:

$$\frac{\mathrm{d}Q_{\mathrm{c}}}{\mathrm{d}\phi} = \frac{\mathrm{d}Q_{\mathrm{c,f}}}{\mathrm{d}\phi} + \frac{\mathrm{d}Q_{\mathrm{c,wall}}}{\mathrm{d}\phi} + h_{\mathrm{in}}\frac{\mathrm{d}m_{\mathrm{c,in}}}{\mathrm{d}\phi} + h_{\mathrm{out}}\frac{\mathrm{d}m_{\mathrm{c,out}}}{\mathrm{d}\phi} + h_{\mathrm{f}}\frac{\mathrm{d}m_{\mathrm{c,f}}}{\mathrm{d}\phi} + h_{\mathrm{leak}}\frac{\mathrm{d}m_{\mathrm{c,leak}}}{\mathrm{d}\phi} - p\cdot\mathrm{d}V \tag{2}$$

where $\mathrm{d}Q_{\mathrm{c,f}}$ is the heat of fuel combustion, $\mathrm{d}Q_{\mathrm{c,wall}}$ is heat exchanged through cylinder walls while following equation members are sensible heat of the media entering and exiting the cylinder and the sensitive heat brought in by the fuel.

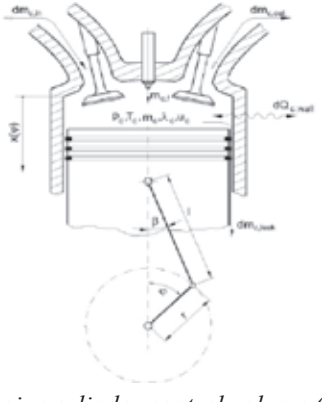

Figure 3: Engine cylinder control volume (Source: [3])

Assuming that the internal energy of the gas is related only to temperature, the equation of the temperature change in the engine cylinder can be written as following:

$$\frac{\mathrm{d}T_\mathrm{c}}{\mathrm{d}\phi}=\frac{1}{m_\mathrm{c}\left(\frac{\partial u}{\partial T}\right)_\mathrm{c}}\left[-p_\mathrm{c}\frac{\mathrm{d}V_\mathrm{c}}{\mathrm{d}\phi}+\sum_\mathrm{i}\frac{\mathrm{d}Q_\mathrm{c,i}}{\mathrm{d}\phi}+\sum_\mathrm{j}h_\mathrm{c,j}\frac{\mathrm{d}m_\mathrm{c,j}}{\mathrm{d}\phi}-u_\mathrm{c}\frac{\mathrm{d}m_\mathrm{c}}{\mathrm{d}\phi}-m_\mathrm{c}\left(\frac{\partial u}{\partial\lambda}\right)_\mathrm{c}\frac{\mathrm{d}\lambda_\mathrm{c}}{\mathrm{d}\phi}\right] \quad (3)$$

The indicated mechanical work of the engine is determined by the expression:

$$\frac{\mathrm{d}W_\mathrm{c}}{\mathrm{d}\phi}=p_\mathrm{c}\frac{\mathrm{d}V_\mathrm{c}}{\mathrm{d}\phi} \quad (4)$$

while pressure in cylinder p_c is determined by the ideal gas state equation:

$$p_\mathrm{c}=\frac{m_\mathrm{c}\cdot R_\mathrm{c}\cdot T_\mathrm{c}}{V_\mathrm{c}} \quad (5)$$

From geometry and kinematics of the crank mechanism, the cylinder volume V_c can be calculated by following expression:

$$V_\mathrm{c}(\phi)=\frac{V_\mathrm{s}}{2}\left[(1-\cos\phi)+\frac{1}{\lambda_\mathrm{m}}\left(1-\sqrt{1-\lambda_\mathrm{m}^2\sin^2\phi}\right)+\frac{2}{\varepsilon-1}\right] \quad (6)$$

where V_s is swept volume, ε is compression ratio and λ_m is rod ratio.

According to analytic terms given in [4] and [2], characteristics of the working fluid depending on gas composition and gas temperature can be determined.

The heat transfer between the working fluid and cylinder walls is given by:

$$\frac{\mathrm{d}Q_\mathrm{c,wall}}{\mathrm{d}\phi}=\sum_\mathrm{i}\alpha_\mathrm{c}\cdot A_\mathrm{c,wall,i}\left(T_\mathrm{wall,i}-T_\mathrm{c}\right)\frac{\mathrm{d}t}{\mathrm{d}\phi} \quad (7)$$

The heat transfer coefficient α_c is determined by empirical expression according to [8]:

$$\alpha_\mathrm{c}=C_1\cdot V_\mathrm{c}^{-0,06}\cdot p_\mathrm{c}^{0,8}\cdot T_\mathrm{c}^{-0,4}\cdot\left(c_\mathrm{MPS}+C_2\right)^{0,8} \quad (8)$$

where coefficients C_1 and C_2 are determined experimentally, and c_MPS is mean piston speed.

A complex process of fuel combustion is usually described by using various numerical models, which can be divided according to [9] and [10] to zero-dimensional, quasi-dimensional and multi-dimensional models. In this paper, the heat release law according to Vibe [11] is applied in terms of crank angle.

According to Vibe, the speed of heat release can be determined using the following term:

$$\frac{x_\mathrm{f}}{\mathrm{d}\phi}=C\ (m+1)\left(\frac{\phi-\phi_\mathrm{IS}}{\phi_\mathrm{CD}}\right)^\mathrm{m}\exp\left(-C\left(\frac{\phi-\phi_\mathrm{IS}}{\phi_\mathrm{CD}}\right)^{\mathrm{m}+1}\right) \quad (9)$$

where x_f is relative amount of fuel combusted, C is constant that depends on fuel combustion efficiency, exponent m is determined as defined in [12], φ_{IS} is crankshaft angle related to the start of the combustion process, and φ_{CD} is crankshaft angle related to the combustion duration. The exponent m was determined according to [12], and the combustion duration φ_{CD} according to [13]. The ignition delay time or angle is calculated using the term given for diesel fuel in [14] and adjusted for heavy fuel oil in [15].

2.2. Exchange of the working fluid in the cylinder of the four-stroke engine

Exchange of the working fluid is conducted by its flow between the cylinder and the intake, i.e. exhaust manifold, and has a significant effect on the engine operation. The flow of the working fluid from one control volume to another is determined by the moment of opening/closing of the valves, by effective flow area and by the pressure difference.

The mass flow of the working fluid which occurs due to the pressure difference, with assumption that the flow is stationary during the observed time, is determined by the following expression:

$$\frac{\mathrm{d}m}{\mathrm{d}\phi} = \alpha_\mathrm{p}\ A_\mathrm{p,geo}\ \psi\ p_1 \sqrt{\frac{2}{R_1 T_1}}\frac{\mathrm{d}t}{\mathrm{d}\phi} = A_\mathrm{p,ef}\ \psi\ p_1 \sqrt{\frac{2}{R_1 T_1}}\frac{\mathrm{d}t}{\mathrm{d}\phi} \tag{10}$$

In described numerical model, geometric flow areas $A_{p,geo}$ of intake and exhaust valves are determined by using appropriate polynomials for approximation of the cam curve of the camshaft. The flow coefficient α_f is determined according the recommendations in [16]. The flow function ψ for subcritical pressure ratio is determined according to [17] as:

$$\psi = \sqrt{\frac{\kappa}{\kappa-1}\left[\left(\frac{p_2}{p_1}\right)^{\frac{2}{\kappa}} - \left(\frac{p_2}{p_1}\right)^{\frac{\kappa+1}{\kappa}}\right]}, \quad \text{if valid:} \quad 1 \geq \frac{p_2}{p_1} \geq \left(\frac{2}{\kappa+1}\right)^{\frac{\kappa}{\kappa+1}} \tag{11}$$

while for supercritical pressure ratio one should use the following term

$$\psi = \left(\frac{2}{\kappa+1}\right)^{\frac{1}{\kappa-1}} \sqrt{\frac{\kappa}{\kappa+1}}, \quad \text{if valid:} \quad \frac{p_2}{p_1} < \left(\frac{2}{\kappa+1}\right)^{\frac{\kappa+1}{\kappa}} \tag{12}$$

where subscript 1 is related to the state in the upstream control volume and subscript 2 is related to the state in the downstream control volume.

2.3. Intake manifold

The turbocharger supplies air to the intake manifold under pressure that depends on the engine load and speed. Before entering the intake manifold, the air is cooled by passing through the cooler, assuming automatic control of the air temperature at the outlet of the cooler.

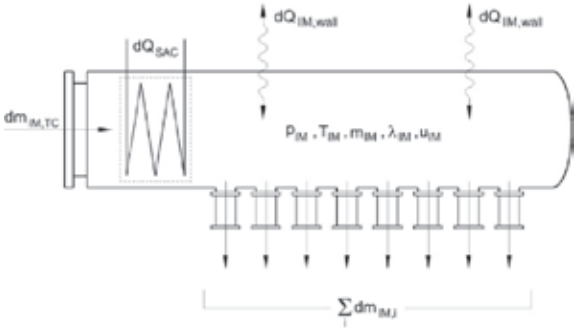

Figure 4: Intake manifold (Source: [3])

The change of air mass in the intake manifold is determined by the expression:

$$\frac{\mathrm{d}m_{\mathrm{IM}}}{\mathrm{d}\phi}=\frac{\mathrm{d}m_{\mathrm{IM,TC}}}{\mathrm{d}\phi}+\sum_{\mathrm{i}}\frac{\mathrm{d}m_{\mathrm{IM,i}}}{\mathrm{d}\phi} \tag{13}$$

During engine operation, the intake manifold volume does not change neither the fuel is burnt within it. Thus, the temperature change in the intake manifold is determined by the expression:

$$\frac{\mathrm{d}T_{\mathrm{IM}}}{\mathrm{d}\phi}=\frac{1}{m_{\mathrm{IM}}\left(\frac{\partial u}{\partial T}\right)_{\mathrm{IM}}}\left[\frac{\mathrm{d}Q_{\mathrm{IM,wall}}}{\mathrm{d}\phi}+\sum_{\mathrm{i}}h_{\mathrm{i}}\frac{\mathrm{d}m_{\mathrm{IM,i}}}{\mathrm{d}\phi}-u_{\mathrm{IM}}\frac{\mathrm{d}m_{\mathrm{IM}}}{\mathrm{d}\phi}-m_{\mathrm{IM}}\left(\frac{\partial u}{\partial \lambda}\right)_{\mathrm{IM}}\frac{d\lambda_{\mathrm{IM}}}{d\phi}\right] \tag{14}$$

The model takes into account the heat exchange through the intake manifold walls and the heat exchange in the intake pipes when the air flows into the engine cylinders. The exchanged heat is determined according to the term:

$$\frac{\mathrm{d}Q_{\mathrm{IM,wall}}}{\mathrm{d}\phi}=\left[\alpha_{\mathrm{IM}}A_{\mathrm{IM}}\left(T_{\mathrm{IM,wall}}-T_{\mathrm{IM}}\right)+\alpha_{\mathrm{IM,a}}A_{\mathrm{IM,a}}\left(T_{\mathrm{IM,wall,a}}-T_{\mathrm{IM}}\right)\right]\frac{\mathrm{d}t}{\mathrm{d}\phi} \tag{15}$$

The heat transfer coefficient in the intake manifold α_{IM} determined according to the expressions in [15], while the heat transfer coefficient in the intake pipes α_{IMP} is calculated according to [6].

2.4. Exhaust manifold

The expressions (16), (18) and (19) for calculation of mass change, temperature and exchanged heat of the intake manifold are also applicable to the exhaust manifold model. The heat transfer coefficient in the exhaust manifold is determined according to the expressions in [15] while heat transfer coefficient in exhaust pipes is determined according to the expressions in [6].

2.5. Turbocharger

In research of a diesel engine operation under steady-state operating conditions, the numerical model of a turbocharger assumes that the air mass flow for a given engine load is known. Engine manufacturers usually provide mass flow data for several operating points ranging from 50 % to 100 % of the engine nominal power.

After compression with the turbocharger, the temperature of the intake air is given by:

$$T_{AC} = T_O + \frac{\left|\Delta h_{C,is}\right|}{\eta_{C,is} \cdot c_{p,air}} \tag{16}$$

while the temperature of the exhaust gases after the turbine may be determined by the following expression:

$$T_{AT} = T_{EM} - \frac{\left|\Delta h_{T,is}\right|}{\eta_{T,is} \cdot c_{p,EG}} \tag{17}$$

2.6. Effective engine power

The indicated engine power is calculated by integrating the total work for all cylinders in one duty cycle as follows:

$$P_{ind} = \frac{n_M}{30\ \tau} \sum_{i=1}^{z} \int \frac{dW_{C,i}}{d\phi}\, d\phi \tag{18}$$

where z is number of cylinders, and n_E is the engine speed expressed in rpm.

The effective engine power can be calculated by using the expression:

$$P_{ef} = \frac{z\ n_M}{30\ \tau} V_S\ p_{MEP} = P_{ind} \frac{p_{MEP}}{p_{MIP}} \tag{19}$$

where p_{MEP} is the mean effective pressure and p_{MIP} is the mean indicated pressure.

The mean effective pressure can be calculated as the difference between the mean indicated pressure and the mean pressure of mechanical losses of the engine mechanism and attached equipment. In the numerical model presented in this paper, the mean pressure of mechanical losses is calculated using approximation terms that are defined in [18].

3. Implementation of zero-dimensional model

During developing and testing the computer program, the data of the Wärtsilä 12V50DF medium-speed four-stroke diesel engine was used. One of the reasons for choosing this engine is the availability of test data from the LNG carrier with diesel-electric propulsion. Although this engine can be used as dual fuel engine, all the data used in the model validation, as well as the numerical model data, were generated when running the engine on heavy fuel oil.

Main Wärtsilä 12V50DF engine data according to [19]:

Cylinder diameter	500 mm
Piston stroke	580 mm
Valves per cylinder	2 intake and 2 exhaust valves
Diameter of intake and exhaust valves	165 mm / 160 mm
Cylinder number and configuration	12 cylinders, Vee of 45°
Nominal RPM	514 min^{-1}
Mean piston speed	9,9 ms^{-1}
Maximum continuous rating	11700 kW
Number of turbochargers	2
Turbocharger type	ABB TPL 71-C

The following is a table of engine performance features according to the engine manufacturer's data and the data collected during the LNG carrier's sea trial voyages before delivery to the client (details of the ship known to the authors)

Table 1: W 12V50 DF engine test data (Source: Wärtsilä)

Engine load	50%	75%	100%
Engine effective power, kW	5850	8775	11700
Specific fuel oil consumption, g/kWh	196	187	189
Exhaust gas temperatures after TC, °C	337	336	352
Exhaust gas mass flow, kg/s	13,9	18,4	23,0

Table 2:. W 12V50 DF engine test data (Source: sea trials)

Engine load	40%	50%	71%
Engine effective power, kW	4680	5850	8307
Specific fuel oil consumption**, g/kWh	199	197	190
Maximum cylinder pressure, bar	70	83	107
Exhaust gas temperatures after TC, °C	412	392	359

*** Specific fuel oil consumption regarding generator load*

All of the above information is related to the operation of the engine while operating the synchronous generator. Based on the available data, simulation of steady-state operation of the engine was performed for five operating points in the range of 40% to 100% of the nominal engine power.

4. Simulation results and their validation

The developed computer program for simulation of steady-state engine operation as a result provides a number of significant data for the analysis of engine operation at different loads. The usability of the program was checked for engine loads ranging from 10% to 110% of nominal power. Some of the simulation results are shown below.

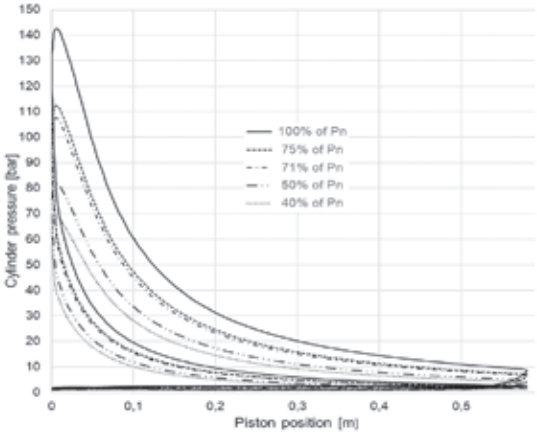

Figure 5: Closed indicating diagrams

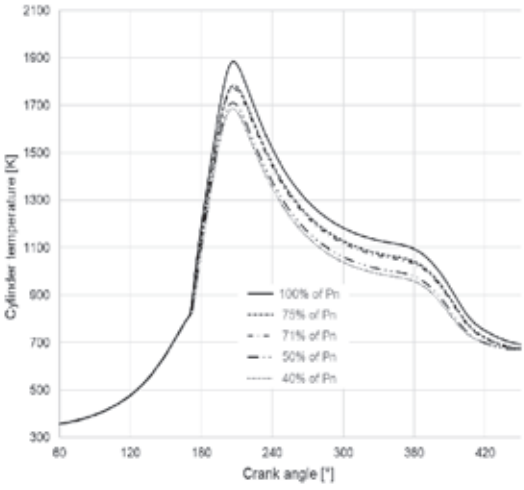

Figure 6: Cylinder temperature variation regarding crank angle

Model validation was performed by comparing the data in Tab. 1 and Tab. 2 with simulation data for specific fuel consumption, maximum cylinder pressure and exhaust gas temperature. In doing so, the data for the five operating points of engine operation were processed as mentioned earlier.

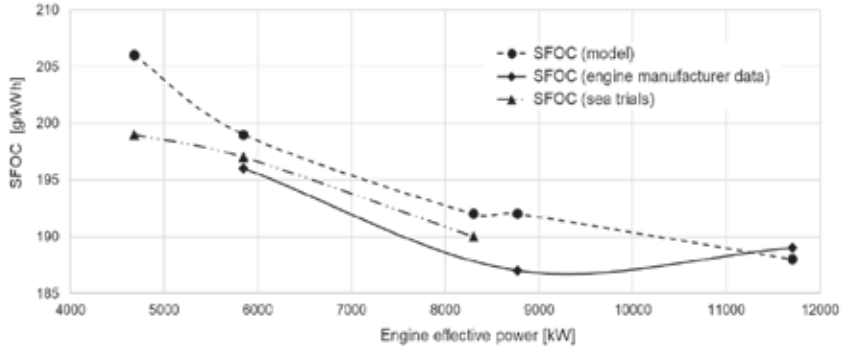

Figure 7: Comparison of measured and calculated specific fuel oil consumption

The diagram shows that the largest deviation between measured and calculated values occurs at 40% of the engine load, which is absolutely 7 g/kWh, or 3.5%, while the smallest difference is in the range from 50% to 71% of the engine load. In that load range, absolute difference is never bigger than 2 g/kWh, or 1.0%.

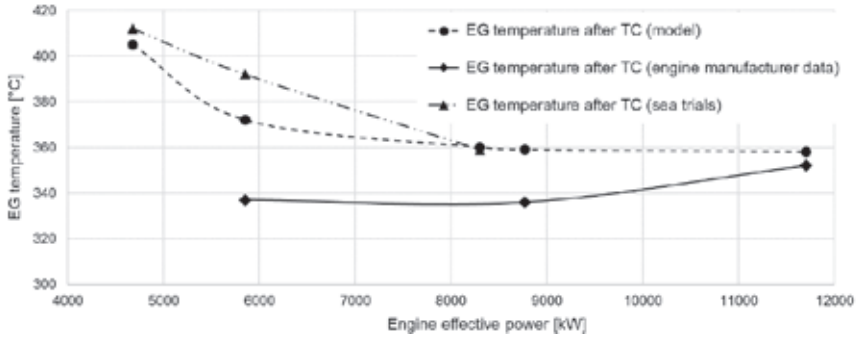

Figure 8: Comparison of measured and calculated exhaust gas temperatures after turbocharger

The diagram shows that the largest deviation of 35 °C or 10,4% occurs at 50% of the engine load. The deviation for the same operating point when comparing the data from the sea trial and those obtained by simulation, deviation is 20 °C or 6,8%. At full engine load, the difference of exhaust gas temperatures after the turbocharger is only 6 °C or 1.7%.

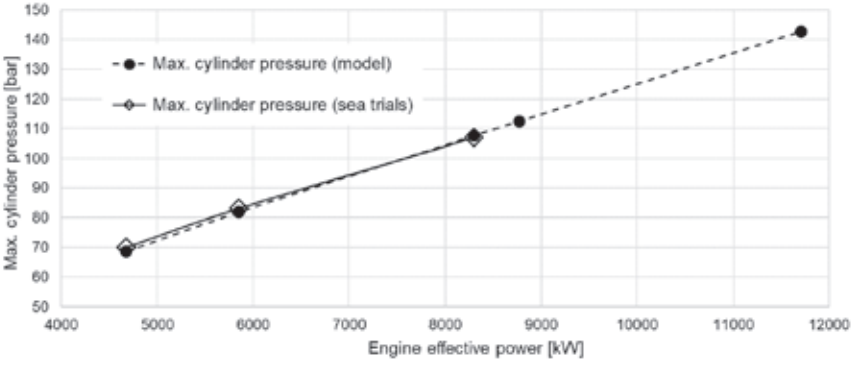

Figure 9: Comparison of measured and calculated maximum cylinder pressure for different engine loads

Comparison of the maximum cylinder pressures occurring at engine load of 40%, 50% and 71% of the rated power shows that the deviations are very small and do not exceed 1 bar. It should be noted that the pressure data from the sea trial indicate an average pressure value that represents the arithmetic mean value for all 12 engine cylinders.

5. Conclusion

The described zero-dimensional model of the four stroke marine diesel engine was developed to investigate the impact of the Miller process, multiple injection and increased turbocharging pressure on engine performances such as specific fuel oil consumption, exhaust gas temperature and nitrogen oxide emissions. The model is primarily intended to simulate the operation of 4-stroke diesel engines at stationary operating conditions, but the modularity of the program allows it to be relatively easy to adapt to non-stationary operating conditions as well as to simulate the operation of 2-stroke slow-speed marine diesel engines.

Achieved results are completely satisfactory considering the possibilities of analysing the operation of the engine and the accuracy of obtained results. Moreover, obtained results and their comparison with the manufacturer's data as well as the data obtained during the sea trial show slight deviations. This confirmed the applicability of the model for research purposes to optimize marine diesel engines. The model calibration was performed on the basis of available data for the Wärtsilä 12V46 engine, and thus the adapted model was used to simulate the operation of the Wärtsilä 12V50DF engine without further adjustments.

It is especially important to point out the negligible variations when comparing the maximum pressures in the engine cylinder and in the case of specific fuel consumption. Slightly larger deviations were observed at the exhaust gas temperature.

It follows from all of the above that the numerical model presented and tested represents a solid basis for continued research in this field, and that the relative simplicity of the model has no significant effect on the accuracy of the results. Created computer program does not allow monitoring of changes in nitrogen oxide emissions so far. The single-zone model will serve as a substrate to which in the second phase the model is upgraded, where the cylinder space is divided into three zones during combustion. In this way, the extended model will allow modelling of nitrogen oxide emissions with satisfactory accuracy.

Acknowledgements

This work has been supported by the Croatian Science Foundation under the project IP-2018-01-3739.

References:

1. Review of maritime transport 2018, UNCTAD, United Nations, 2018.
2. Medica, V.: Simulation of turbocharged diesel engine driving electical generator under dynamic working conditions, Doctoral thesis, Faculty of Engineering, Rijeka, 1988.
3. Mrakovčić, T.: Osnivanje i vođenje brodskog pogonskog postrojenja primjenom numeričke simulacije, Doktorska disertacija, Rijeka, 2003.
4. Woschni, G.: Die Berechnung der Wandverluste und thermischen Belastung der Bauteile von Dieselmotoren, MTZ 31 (1970) 12, 491-499 (42).
5. Jankov, R.:, Matematičko modeliranje strujno-termodinamičkih procesa i pogonskih karakteristika dizel-motora, Naučna knjiga Beograd, 1984., I i II dio.
6. Pflaum, W., Mollenhauer, K.: Wärmübergang in der Verbrenungs-kraftmaschine, Springer Verlag, Wien, 1977. (83).
7. Löhner, K., Döhring, E., Chore, G.: Temperaturschwingungen an der Innenwand von Verbrennungskraftmaschinen, MTZ Nr. 12, 1956.
8. Hohenberg, G.: Advanced approaches for Heat Transfer Calculation, SAE Paper 790825, 1979.
9. Heywood, J., B.: Engine Combustion modelling - An Overview, Symposium on Combustion Modelling, GMC Research Labs., 1980. (113).
10. Boulochos, K., Papadopulos, S.: Zur Modellbildung des motorischen Verbrennungsablaufes, MTZ 45 (1984) 1, 21-26 (144).
11. Vibe, I. I.: Brennverlauf und Kreisprozess von Verbrenungsmotoren, VEB Verlag Technik, Berlin, 1970.
12. Woschni, G. Anisits, F.: Eine methode zur vorausberechnung der änderung des brennverlaufes mittelschnellaufender dieselmotoren bei geänderten betriebsbedingungen, MTZ 34 (1974) 4, 106-115.
13. Betz, A. Woschni, G.: Umsetzungsgrad und brennverlauf aufgeladener dieselmotoren im instationären betrieb, MTZ 47 (1986) 7/8, p.263-267.
14. Sitkei, G.: Über den dieselmotorischen Zündverzug, MTZ 24 (1963), 6, 190-194.
15. Boy, P.: Beitrag zur Berechnung des instationären Betriebsverhaltens von mittelschnellaufenden Schiffsdieselmotoren, Dissertation, Hannover, TH, 1980.
16. Chapman, K.: Engine Airflow Algorithm Prediction, Introduction to Internal Combustion Engines, Kansas State University, 2001.
17. Bošnjaković, F.: Nauka o toplini II, IV izdanje, Tehnička knjiga, Zagreb, 1976.
18. MAASS, H., KLIER, H.: Kräfte, Momente und deren Ausgleich in der Verbrennungskraftmaschine, Springer-Verlag, Wien - New York 1981.
19. Wärtsilä 50DF Product Guide - a19 - 25 July 2018.